Disentangling abiotic and biotic effects of treated wastewater on stream biofilm resistomes enables the discovery of a new planctomycete beta-lactamase

Mustafa Attrah[1,2+], Milo R. Schärer[1+], Mauro Esposito[1*], Giulia Gionchetta[3], Helmut Bürgmann[3], Piet N.L. Lens[2,4], Kathrin Fenner[5,6], Jack van de Vossenberg[2], Serina L. Robinson[1*]

[+]co-first authors contributed equally to this work

*corresponding author: serina.robinson@eawag.ch

[1]Department of Environmental Microbiology, Eawag, Swiss Federal Institute of Aquatic Science and Technology (Eawag), 8600 Dübendorf, Switzerland

[2]Water Supply, Sanitation and Environmental Engineering, IHE Delft Institute for Water Education, Westvest 7, 2611 AX Delft, The Netherlands

[3]Department of Surface Waters - Research and Management, Eawag, Swiss Federal Institute of Aquatic Science and Technology, 6047 Kastanienbaum, Switzerland

[4]National University of Ireland Galway, University Road, Galway H91 TK33, Ireland

[5]Department of Environmental Chemistry, Eawag, Swiss Federal Institute of Aquatic Science and Technology (Eawag), 8600 Dübendorf, Switzerland

[6]Department of Chemistry, University of Zürich, 8057 Zürich, Switzerland

Abstract

Background

Antibiotic resistance, which is mediated by environmental reservoirs, poses a threat to human and animal health. Aquatic biofilms impacted by treated wastewater (WW) are known environmental reservoirs for antibiotic resistance, however the specific influence of biotic factors and abiotic factors from WW on the abundance of antibiotic resistance genes (ARGs) within aquatic biofilms remains unclear. Additionally, experimental evidence is limited as to whether genes with low sequence similarity to reference ARGs actually encode for functional ARGs, particularly within complex aquatic microbial communities.

Results

To disentangle the effects of abiotic and biotic factors on ARG abundances, natural biofilms were previously grown in flume systems with different proportions of stream water and either ultrafiltered or nonultrafiltered WW. In this study, we conducted deep shotgun metagenomic sequencing of 75 biofilm, stream, and WW samples from these flume systems and compared the taxonomic and functional microbiome and resistome composition. Statistical analysis revealed an alignment of the resistome and microbiome composition and a significant association with experimental treatment. Several ARG classes exhibited an increase in metagenomic abundances in biofilms grown with increasing percentages of nonultrafiltered WW. In contrast, sulfonamide and BEL family beta-lactamase ARGs showed greater abundances in biofilms grown in ultrafiltered WW compared to nonultrafiltered WW. Overall, our results pointed toward the dominance of biotic factors over abiotic factors in determining ARG abundances in WW-impacted stream biofilms and suggested gene family-specific mechanisms for ARGs which exhibited divergent abundance patterns. To investigate one of these specific ARG families experimentally, we biochemically characterized a new beta-lactamase from the *Planctomycetota*

(*Phycisphaeraceae*). This beta-lactamase displayed activity in the cleavage of cephalosporin analog despite sharing low sequence identity with known ARGs.

Conclusions

This discovery of a functional planctomycete beta-lactamase ARG is noteworthy, not only because it was the first beta-lactamase to be biochemically characterized from this phylum, but also because it was not detected by standard homology-based ARG tools. In summary, this study conducted metagenomic analysis on the relative importance of biotic and abiotic factors in the context of WW discharge and their impact on both known and new ARGs in aquatic biofilms.

Keywords

Antibiotic resistance genes, Stream resistomes, Biofilms, Flume systems, Wastewater effluent, Metagenomics, Sulfonamides, Planctomycetota, AlphaFold2, Beta-lactamases

Background

Antibiotic resistance is a major threat to public health. Among the numerous factors contributing to antibiotic resistance, anthropogenic pollution plays a role in altering the abundance and prevalence of antibiotic resistance genes (ARGs) in environmental reservoirs [1–4]. The rapid increase in the consumption of antibiotics and release of micropollutants (MPs) into the environment stimulates the spread of antibiotic-resistance genes (ARGs), posing a threat to modern medical procedures and treatments that rely on effective antibiotics [5].

Aquatic ecosystems that receive effluent from wastewater treatment plants (WWTPs) are influenced by biotic factors, such as antibiotic-resistant bacteria released from WWTPs [6] and abiotic factors [7,8] including nutrients and MPs that are not completely eliminated by conventional WWTPs [9]. Several recent studies have demonstrated that exposure to WWTP effluent alters

71 the taxonomic and ARG compositions of microbial communities in downstream rivers [10–14].
72 However, disentangling the effects of abiotic and biotic factors on ARG abundance is challenging
73 in the environment. Here, to systematically distinguish abiotic and biotic factors, we built on a
74 previous research study in which controlled flume systems were used to grow biofilms in
75 ultrafiltered and nonultrafiltered WWTP effluent diluted with different proportions of stream water
76 [10,11]. Ultrafiltration (UF) treatment (pore size 0.4 μm) removed most of the microorganisms and
77 particles (biotic factors) while maintaining consistent nutrient and MP levels, including antibiotics.
78 Therefore, separating biotic factors from abiotic factors in UF treatment enabled investigation of
79 the factors shaping the 'resistome', i.e., the total composition of antibiotic resistance genes
80 (ARGs), of stream biofilms influenced by WWTP discharge.
81
82 Many studies on stream biofilms have relied on amplicon sequencing methods for taxonomic
83 and/or ARG profiling [10,15–17]. In contrast to amplicon sequencing, short-read and long-read
84 shotgun metagenomic sequencing studies of streams and stream biofilms [13,18,19] do not
85 introduce polymerase chain reaction (PCR) amplification bias. As we demonstrated in this study,
86 PCR-free metagenomic sequencing also enables the identification of sequence-divergent ARGs
87 not detected by conventional primer pairs. Amplicon sequencing is more sensitive because it can
88 aid in the detection of low abundance species, but it is also biased toward the amplification of
89 specific taxa during PCR [20,21]. Specifically, PCR bias limits the detection of some bacterial
90 phyla such as the *Planctomycetota*, for which the commonly-used 16S rRNA PCR primers do not
91 properly bind [22,23]. The *Planctomycetota* are undersampled by classical amplicon-based
92 methods [23] and are a focus in this study because of their relevance in WWTP [24], lacustrine
93 [25], and riverine biofilm (periphyton) communities [26]. We conducted deep shotgun
94 metagenomic sequencing of stream biofilms and water samples in this study, which enabled us
95 to sample less well-studied microorganisms and their functional genes including ARGs.

96 Here, we demonstrated a combined computational and biochemical workflow to investigate the
97 effects of treated wastewater (WW) on the microbiome taxonomic composition, functional enzyme
98 diversity, and ARG abundance in flume biofilms grown in natural stream water mixed with different
99 proportions of ultrafiltered and nonultrafiltered WW [10,11]. Specifically, we leveraged the
100 functional genes identified through shotgun metagenomic sequencing to heterologously express
101 and purify an uncharacterized ARG from the phylum *Planctomycetota*. Despite sharing low
102 sequence identity with computationally-identified ARGs, the enzyme displayed beta-lactamase
103 activity. Overall, this study enabled the dissection of biotic and abiotic factors which affect stream
104 biofilm resistomes and led to the characterization of both known and new ARGs.

105 Methods

106 **Biofilm cultivation and sampling**

107 The flume systems and biofilm cultivation procedures used in two independent experiments to
108 generate the samples sequenced in this study were described previously [10,11]. Briefly, the
109 system consisted of flow-through channels fed with different mixtures of two different water
110 sources: (1) a peri-urban stream (Chriesbach; Dübendorf, Switzerland) and (2) treated
111 wastewater from a pilot-size wastewater treatment plant (100-person equivalents). In the first
112 experiment (Exp. 1), the stream water was mixed with treated wastewater (WW) at the following
113 percentages: 0% (control), 10%, 30%, and 80% WW. In the second experiment (Exp. 2), the 10%
114 treatment was omitted and replaced by additional treatments with 30% and 80% ultrafiltered WW
115 (UF) using a filter with a pore size of 0.4 µm to remove particles, e.g., suspended solids and
116 microorganisms. Glass slides were added to the flow-through channels, and biofilms that naturally
117 formed on the slides were allowed to develop for a period of four weeks. Water parameters (pH,
118 temperature, conductivity, dissolved oxygen) were monitored weekly [10,11].

119

120 **DNA extraction and metagenomics assessment**

121 Stream water, WW and UF WW, and biofilms from glass slides were sampled as described
122 previously [11,27]. Total genomic DNA was extracted with a DNeasy PowerBiofilm Kit (QIAGEN)
123 for a total of 75 samples (**Table S1**). The quality and quantity of the DNA extracts were measured
124 using a NanoDrop One spectrophotometer. Extracted DNA samples were stored at -20°C and
125 shotgun metagenomic sequencing was performed using the Illumina platform NovaSeq with a
126 paired-end (2×150 bp; an average of 20 Gbp raw data per sample) strategy. Library construction
127 and sequencing was performed by Novogene (Cambridge, UK). The reads obtained from shotgun
128 metagenomics and those containing adapters and low-quality reads (N > 10% and quality score
129 ≤ 5) were removed by Novogene, and the read qualities were double-checked by the authors
130 using Fastp v.0.20.0 (https://github.com/OpenGene/fastp). De novo assembly was performed
131 using MEGAHIT v1.2.9 [28]. Open reading frames (ORFs) were predicted from the assembled
132 contigs using Prodigal v2.6.3 [29]. Although metagenomes from both Exp. 1 and Exp. 2 were
133 sequenced and the data for both were deposited, we focused on Exp. 2 for the analyses reported
134 here since Exp. 2 included UF treatments, unlike Exp. 1.

135

136 **Taxonomic and functional profiling**

137 The taxonomic composition of the metagenomes was profiled using the degenerate consensus
138 marker gene profiling tool, mTAGs v1.0.4, with 1000 maximum accepts and 1000 maximum
139 rejects [30,31]. The mTAGs profiles for all samples were merged using mTAGs merge function.
140 Genus- and phylum-level per-sample count tables were used for subsequent analysis. Counts
141 corresponding to Enzyme Commission (EC) Number classes were compiled as described
142 previously [32]. Briefly, fourth-level EC number counts were calculated using the EC-annotated
143 prokaryotic fraction of the UniProt database using DIAMOND blastx v2.0.6 [33] and a minimum
144 bitscore cutoff of 50 (all other parameters set to default).

145

146 **Reads-based ARG detection and ordination analyses**

147 The ARG resistome was profiled using the DeepARG v1.0.2 short reads pipeline with default
148 settings [34]. ARG counts normalized by the 16S-rRNA counts within the output files for each
149 sample were merged into an abundance table. All data were analyzed and visualized in R v4.3.0
150 with the tidyverse package [35]. Principal coordinate analysis (PCoA) of the microbiome
151 composition was performed using the genus abundance table. Unaligned and unassigned reads
152 were removed. Genus counts were normalized using the trimmed mean of M-values (TMM)
153 method within the EdgeR package [36–38]. Normalized genus counts were square-root-
154 transformed. PCoA of the resistome composition was calculated from 16S-normalized DeepARG
155 abundances [34]. PCoA analysis of functional enzyme composition was calculated from
156 normalized and Hellinger-transformed EC numer counts. For all the data sets, pairwise Bray-
157 Curtis distances between samples were computed using the 'vegdist' function from the vegan
158 package [39]. PCoA was performed using the 'pcoa' function from the ape package [40].
159 Procrustes analysis comparing the PCoA vectors was conducted using the 'procrust' and 'protest'
160 functions from the vegan package [39]. The Kruskal-Wallis test (McKnight and Najab, 2010) was
161 applied to test for significant correlations between the normalized average coverage of different
162 ARGs and wastewater effluent proportions (WW%), and p-values were corrected for multiple
163 hypothesis testing using the Benjamini-Hochberg method [41].

164

165 **ARG identification and coverage analysis from metagenome assemblies**

166 For a complementary and separate approach to the metagenomic short reads pipeline for ARG
167 analysis, predicted open reading frames (ORFs) from assembled metagenomes were identified
168 by protein BLAST v2.9.0 [42] search against the Structured Antibiotic Resistance Genes (SARG)
169 protein database v2.2, with stringent e-values and query coverage cutoffs of 0.1 and 20,

170 respectively [43]. Using thresholds established previously in similar samples [44] for the detection
171 of ARGs in riverine metagenomes, BLAST hits with more than 85% amino acid identity and an
172 alignment length of 100 amino acids were retained. BLAST hits were then clustered using CD-
173 HIT v4.6.8 [45,46], with parameters –n 5 and –c 0.7. The 102 non-singleton cluster
174 representatives of SARG hits were selected for further analysis. Metagenomic coverage of
175 selected ARG cluster representatives were calculated across all metagenomes based on
176 methods previously described [44]. Briefly, raw reads were mapped back to BLAST hits using
177 Bowtie2 v2.4.4 [47] with the parameters shown in **Table S2**. Coverage depth was calculated using
178 samtools v1.12 and average coverage was calculated as described previously [48]. The average
179 coverage of the resulting 102 ORFs was normalized to reads per million as previously described
180 [44].
181
182 **Bioinformatic analyses of beta-lactamases**
183 Metallo-beta lactamase fold proteins were identified by querying assembled proteins from the 75
184 metagenomes and additional publicly-available metagenomes from MP enrichment studies (NCBI
185 accession: PRJNA725625) using BLAST v.2.9.0 [49] with relaxed parameters (e-value = 0.1,
186 qcov_hsp_perc = 20, all other parameters set to default) to detect homologs with low sequence
187 identity to known ARGs. Taxonomic diversity and trends in abundances of metallo-beta lactamase
188 fold homologs across different WW and UF WW conditions were examined leading to the
189 prioritization of two metallo beta-lactamase homologs (NCBI accession numbers MBX3358097.1
190 and MBX3359331.1) for experimental characterization. Structural modeling of MBX3358097.1
191 was conducted using ColabFold AlphaFold 2.0 [50] with default parameters. AlphaFold models
192 were assessed for quality based on predicted local distance difference test (pLDDT) scores and
193 aligned pairwise with the reference structure in the Protein Data Bank (PDB ID: 3NKS) using the
194 PyMOL ‘super’ command with default parameters.

195

196 **Cloning and protein expression**

197 For functional characterization, two full-length *Phycisphaeraceae* (*Planctomycetota*) proteins
198 (NCBI accession numbers MBX3358097.1 and MBX3359331.1) were codon-optimized for *E. coli*
199 codon usage using the Integrated DNA Technologies Codon Optimization Tool
200 (https://eu.idtdna.com/pages/tools/). Signal peptides were detected using SignalP v6.0 [51] and
201 removed where present (**Table S3**). The genes were synthesized as gBlocks by Integrated DNA
202 Technologies. The genes were cloned individually by Gibson Assembly into the multiple cloning
203 site 1 of the pETDuet-1 vector (*ampR* resistance marker) with N-terminal hexahistidine tags
204 (**Table S3**). The constructs were transformed into *E. coli* DH5α cells and verified by Sanger
205 sequencing (Microsynth, Balgach, Switzerland). The sequence-verified constructs were
206 subsequently transformed into *E. coli* BL21(DE3) cells (New England Biolabs Frankfurt,
207 Germany). Starter cultures (5 mL) were grown in LB with 100 µg/ml ampicillin overnight at 37°C.
208 From the starter cultures, 2.5 mL was added to 400 mL LB with 100 µg/mL ampicillin in a 1 L
209 baffled Erlenmeyer flask and grown to an optical density of 0.5-0.8 at 37°C. Protein expression
210 was induced by adding 0.1 mM isopropyl β-D-1-thiogalactopyranoside (IPTG) and cultures were
211 incubated for 18 h at 16°C.

212

213 **Protein purification**

214 Expression cultures were poured into 50 mL Falcon tubes and centrifuged at 4000 rcf for 15 min.
215 Supernatants were decanted, and cell pellets were resuspended in 4 mL buffer A (20 mM Tris,
216 500 mM NaCl, 20 mM imidazole, 10% glycerol, pH = 8) per gram of pellet weight. Cells were lysed
217 by 2 cycles of sonication using a 6 mm needle, 20% amplitude and 10 x 10 second pulses with a
218 rest time of 10 seconds in between (total sonication time per cycle = 3 minutes). Lysates were
219 centrifuged at 20,000 rcf at 4°C for 1h. Cleared lysate was filtered through a 0.2 µm syringe filter,

220 loaded into a ÄKTA Pure system (Cytiva Europe GmbH, Glattbrugg, Switzerland) and injected
221 onto a HisTrap FF 5 mL column (Cytiva, Europe GmbH, Glattbrugg, Switzerland). The column
222 was washed with 20 column volumes of buffer A. His-tagged proteins were eluted in 3 column
223 volumes of buffer B (same as buffer A but with an imidazole concentration of 500mM), and 8 × 2
224 mL fractions were collected. The fractions with the highest protein concentrations were
225 determined qualitatively by Bradford assay [52]. Imidazole was removed by running the sample
226 over a PD-10 desalting column (Cytiva Europe GmbH, Glattbrugg, Switzerland) and eluting in
227 buffer (5 mM Tris, 30 mM NaCl, 10% glycerol, 0.1 mM $ZnCl_2$, pH = 8). $ZnCl_2$ was added because
228 the enzyme of interest is suspected to be Zn^{2+} dependent. The purified protein was flash frozen
229 using liquid nitrogen in 200 µl aliquots and subsequently stored at -80°C.
230
231 **β-Lactamase activity assay**
232 The purified, soluble protein (MBX3358097.1) was tested with standard β-lactamase activity
233 detection assays using the chromogenic cephalosporin analog, nitrocefin (Sigma Aldrich) [53].
234 Nitrocefin solutions were prepared in a 40 mM stock solution in DMSO and then diluted in 20 mM
235 Tris buffer (pH = 7.0) immediately before use in a 1 mM working solution. Briefly, standard
236 nitrocefin assays were performed in a 96-well plate by combining 180µl 20 mM Tris buffer with
237 0.1 mM $ZnCl_2$ (pH = 7.0) with 10 µL purified enzyme and 10µL nitrocefin working solution. The
238 plate was incubated in a plate reader (BioTek Synergy H1, Agilent) at 25°C, and the absorbance
239 at 482 nm was measured every minute for 2 h. As negative controls, boiled enzyme and buffer-
240 only conditions were included in every assay. To obtain the boiled enzyme control, aliquots of
241 purified protein were incubated at 100°C for 15 minutes. Reaction rates were quantified from
242 continuous measurements as described previously by Ryu et al. using the molar extinction
243 coefficient of nitrocefin (12,124 M^{-1} cm^{-1}) in 20 mM Tris [54].

Results and discussion

Biotic factors are more dominant than abiotic factors for altering the taxonomic and functional composition of biofilms grown in WWTP effluent

We deeply sequenced metagenomes from a total of 75 biofilm and water samples to an average sequencing depth of 138 million reads per sample (max. 204 million reads). After metagenomic assembly, we analyzed the taxonomic composition of stream biofilm communities to assess whether community composition was correlated with different experimental treatments: 30% WW, 80% WW, 30% UF WW, 80% UF WW, or stream water (0% WW). Experimental treatment was correlated with taxonomic composition for both prokaryotes (PERMANOVA, $R^2 = 0.65$, $p < 0.001$) (**Figure 1**) and eukaryotes (PERMANOVA, $R^2 = 0.70$, $p < 0.001$) (**Figures S1-S3**) at the genus level [30]. Growth in 80% WW relative to stream water (0% WW) altered prokaryotic biofilm community composition, namely we observed a decrease in the relative abundance of *Cyanobacteria* and *Verrucomicrobiota* and an increase in the relative abundance of *Bacteroidota* (**Figure 1**), in agreement with previous 16S rRNA gene-based analysis [27]. These shifts also mirror changes in microbial communities downstream of WWTPs relative to communities upstream [14]. However, these previous field studies did not include ultrafiltration treatment. We therefore compared WW UF and non-UF WW-grown bioiflms, and identified several bacterial phyla which showed significant shifts in relative abundance, namely a significant decrease in *Myxococcota* and an increase in *Planctomycetota* (**Figure 1**). UF treatment therefore altered microbial community composition including taxa with specific relevance for WWTP processes. For example, *Planctomycetota* is the only known phylum capable of anaerobic ammonia oxidation (anammox) for nitrogen removal from WW [25,55,56].

267 The taxonomic composition of biofilms grown in UF WW was more similar to that of biofilms grown
268 in 0% WW than to biofilms grown in non-UF WW, suggesting that biotic factors from WWTPs play
269 a greater role in changes in the stream biofilm community than abiotic factors (**Figure 2, Figure**
270 **S3**). Metagenomic taxonomic analysis demonstrated that WW alters stream biofilm composition,
271 supporting previous studies that some microorganisms from WW are able to colonize and modify
272 biofilm community composition [27]. To leverage the shotgun metagenomic data, we investigated
273 whether treatment also altered the composition of functional enzyme diversity (see Methods).
274 PCoA revealed that the functional enzyme composition (**Figure S4**) was also significantly
275 associated with the experimental treatment (PERMANOVA, $R^2 = 0.58$, $p < 0.001$).

276

277 **Resistome composition correlates with microbiome composition**

278 We next examined how the total set of ARGs detected in each sample - the 'resistome' - varied
279 with experimental treatment (e.g., WW% and non-UF vs. UF). Resistome composition was
280 significantly affected by experimental treatment (PERMANOVA, $R^2 = 0.60$, $p < 0.001$), similar to
281 functional enzyme and taxonomic microbiome composition (**Figure S5**). Biofilms exposed to 30%
282 or 80% UF WW clustered with 0% WW samples as opposed to samples exposed to equivalent
283 amounts of non-UF WW (**Figure 2**).

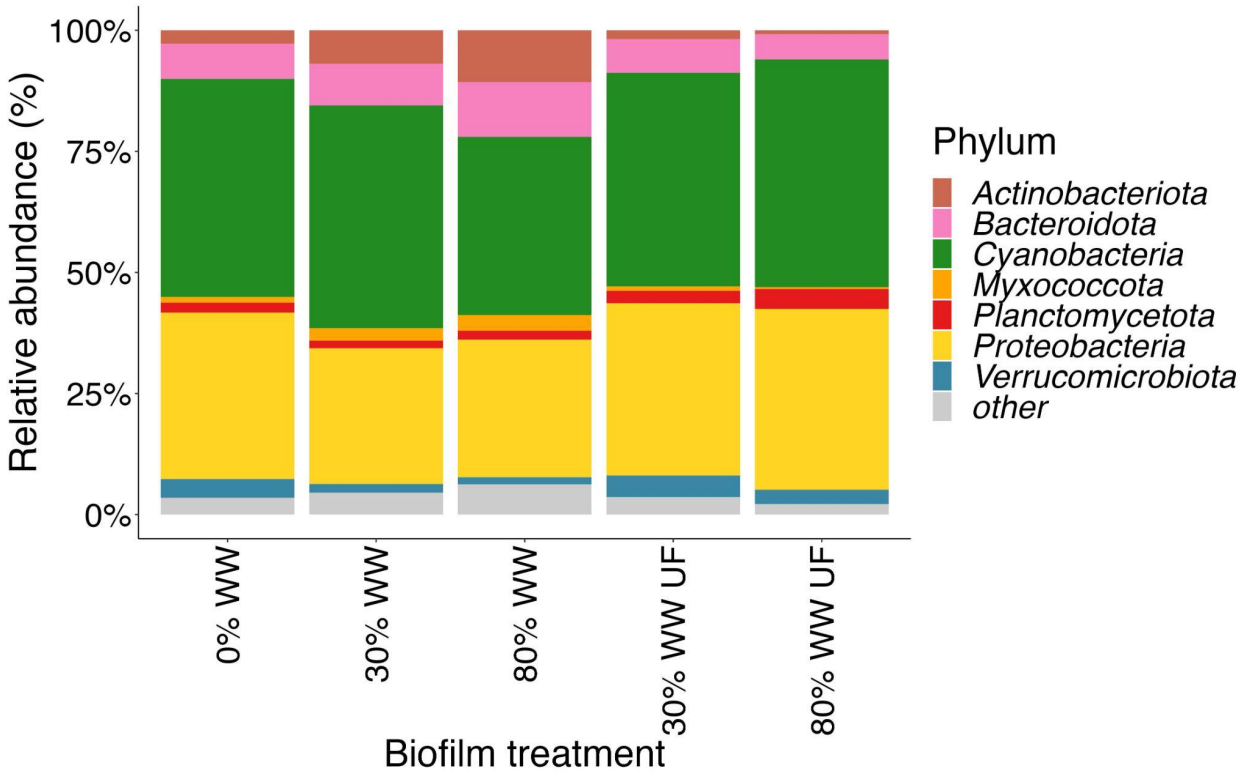

Figure 1. Mean relative abundance of prokaryotic phyla in the metagenomes of stream biofilms. Taxonomic shifts are shown for biofilms which were grown for four weeks continuously in stream water mixed with treated wastewater (WW) with or without ultrafiltration (UF) treatment. Taxa that were in the upper decile of abundance in at least one experimental treatment were retained while the remaining phyla were binned as 'other'.

To test for a relationship between the microbiome and resistome composition, we used Procrustes superimposition of resistome PCoA vectors onto prokaryotic microbiome PCoA vectors (**Figure 2**). Procrustes analysis revealed that the composition of the resistome was structurally related to the composition of the prokaryotic microbiome. The low Procrustes sum of squares of 0.1889 and calculated correlation value of 0.9 in a symmetric Procrustes rotation (p-value < 0.001) indicated a strong alignment between the resistome and microbiome. Similarly, functional enzyme composition was also associated with the resistome composition (**Figure S6,** Procrustes corr. coeff. = 0.89, p-value < 0.001). Alignments between the microbiome and resistome composition

298 has been previously observed in microbial communities downstream of WWTPs [13,14], but local
299 environmental features at different sampling sites are potential confounding factors that may have
300 determined both microbiome and resistome composition in the field. Here, we demonstrated a
301 microbiome-resistome relationship in a controlled experiment with biofilms grown in a defined
302 gradient of stream water to WW and ultrafiltered WW matrices. Generally, the rotated PCoA
303 vectors for the resistome are closer to the prokaryotic microbiome PCoA vectors for biofilm
304 samples than they are for water samples (**Figure 2**). These results further suggest that changes
305 in resistome composition in WW-impacted stream biofilms are likely due to changes in the biofilm
306 communities by WWTP bacteria such as by colonization [27,57].

307

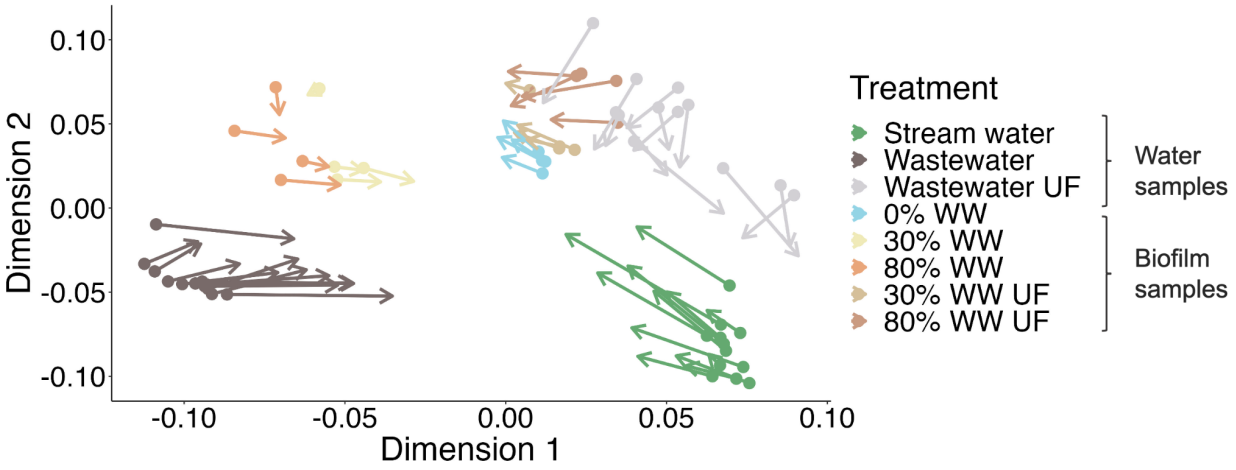

308

309 **Figure 2**. **PCoA-based Procrustes analysis showing a structural alignment between**
310 **microbiome and resistome composition.** Points indicate positions on PCoA axes 1 and 2 of
311 prokaryotic composition (microbiome), while arrow tips indicate positions on PCoA axes 1 and 2
312 of resistome composition following Procrustes rotation. The correlation coefficient in a symmetric
313 Procrustes rotation was 0.901, the sum of squares (m12 squared) was 0.1889), and the p-value
314 was less than 0.001.

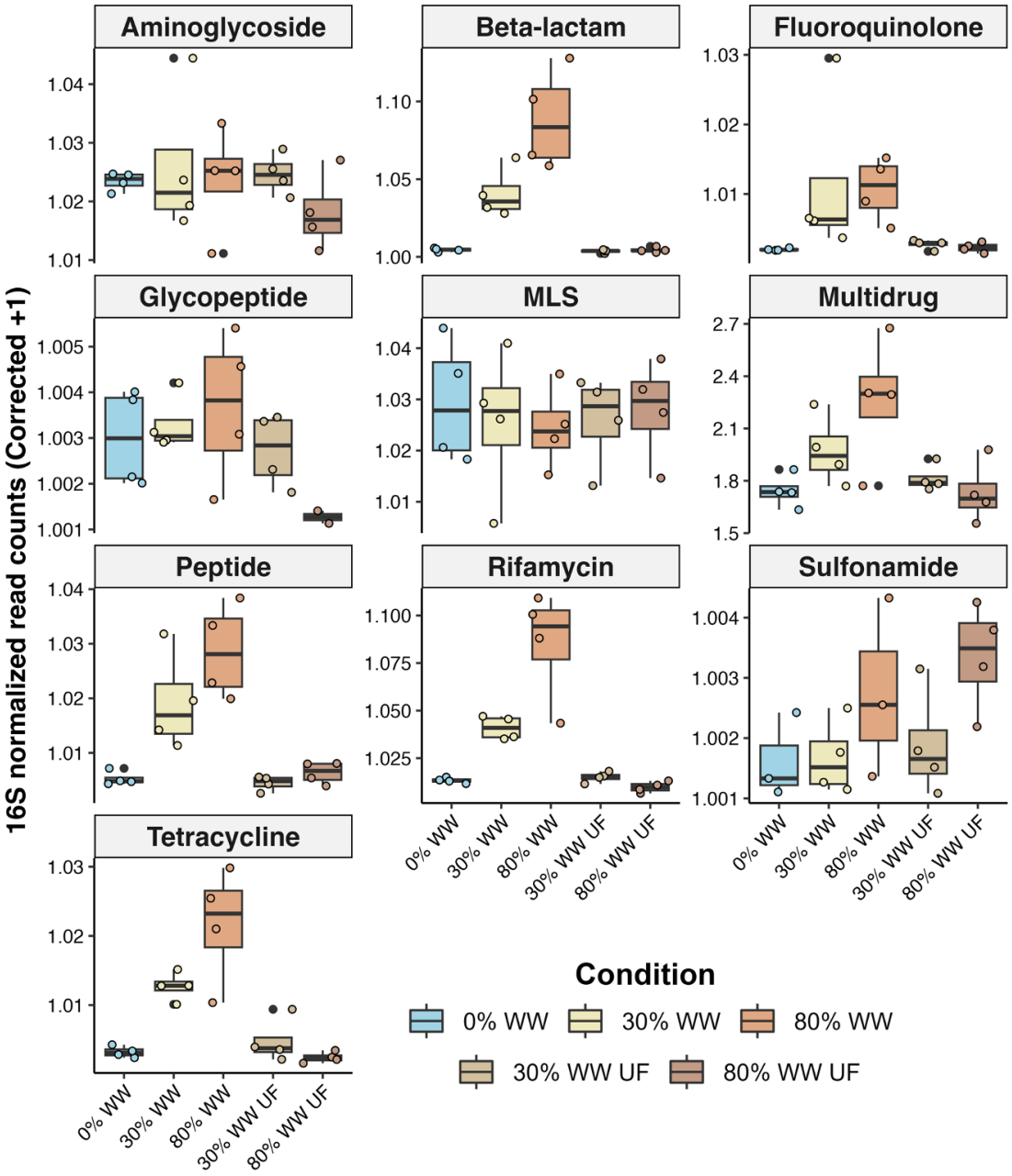

Figure 3. Significant ARG classes profiled using a metagenomic short reads pipeline. Abundance (16S-normalized read counts) of the DeepARG hits assigned to ARG classes that varied significantly with adjusted p-values ≤ 0.001 (Kruskal-Wallis test + Benjamini-Hochberg multiple hypothesis correction) between different treatment conditions. MLS = macrolide-lincosamide-streptogramin.

318 **WW ultrafiltration treatment has ARG class-specific effects on biofilm resistomes**

319 A total of 570 ARGs across 41 different higher-level ARG classes were identified in the biofilm
320 metagenomes using a short reads pipeline for ARG detection [34]. In biofilms, the abundances of
321 ARGs conferring multidrug resistance, in addition to ARGs conferring resistance to beta-lactams,
322 fluoroquinolones, peptides, rifamycins, and tetracyclines, differed significantly between conditions
323 **(Table S5)**.

324

325 The normalized read counts of several, but not all, ARG classes increased with increasing WW%,
326 as shown in **Figure 3**. In contrast, the metagenomic abundances of ARG classes did not increase
327 in biofilms grown in comparable percentages of UF WW with the exception of sulfonamide AR Gs
328 (**Figure 3**). These UF treatment results therefore suggest biotic factors primarily alter the
329 abundances of ARGs in WW-grown biofilms.

330

331 As a notable exception, sulfonamide ARGs exhibited increasing abundance with increasing WW%
332 yet they displayed the highest abundance under 80% UF WW conditions, suggesting a
333 contribution from abiotic factors such as nutrients or micropollutants (MPs) in WW. The high
334 abundance of sulfonamide ARGs in UF-grown biofilms may also be related to gene family-specific
335 mobility mechanisms such as extracellular genetic material which is small enough to pass through
336 the UF membrane. In support of this hypothesis, the sulfonamide ARGs *sul1-4* are known to be
337 highly mobilized in WWTP effluent microbiomes [58]. Although many ARGs are mobile, *sul1*
338 ARGs are known for their pervasive colocalization within class 1 integrons [44] enabling bacteria
339 to acquire and swap sulfonamide resistance genes [59,60]. Analysis of the assembled
340 metagenomic contigs in our samples revealed that *sul1* genes were frequently colocalized on the
341 same metagenomic contigs as mobile genetic elements, including *int1* integron integrases, as
342 well as recombinases and transposases (**Figure S7**). Critically, the presence of *intI1* genes in

343 environmental samples has been suggested as a gene proxy for estimating the levels of
344 anthropogenic pollution, including MPs, as proposed by Gillings et al. [60]. The high abundance
345 of sulfonamide ARGs observed in UF WW-grown biofilms supports the relationship between *int1*
346 genes, sulfonamide ARGs typically associated with *int1,* and abiotic factors, including pollutants
347 [59].

348 **Associations between assembled ARG abundances and WW percentages**

349 Metagenomic assembly-based approaches are likely to have lower sensitivity but higher
350 specificity than short read-based approaches in the detection of antibiotic resistance genes
351 [61,62]. Therefore, as a complementary analysis to the DeepARG short read-based detection
352 methods, we used stringent criteria (see Methods) to query our assembled metagenomes against
353 the Structural Antibiotic Resistance Genes (SARG) database [43]. The query yielded 2,240 hits
354 that clustered at the 70% amino acid sequence similarity level into 102 ARG 'cluster
355 representatives.' Analysis by ARG class resulted in the following ARG cluster counts: 15 beta-

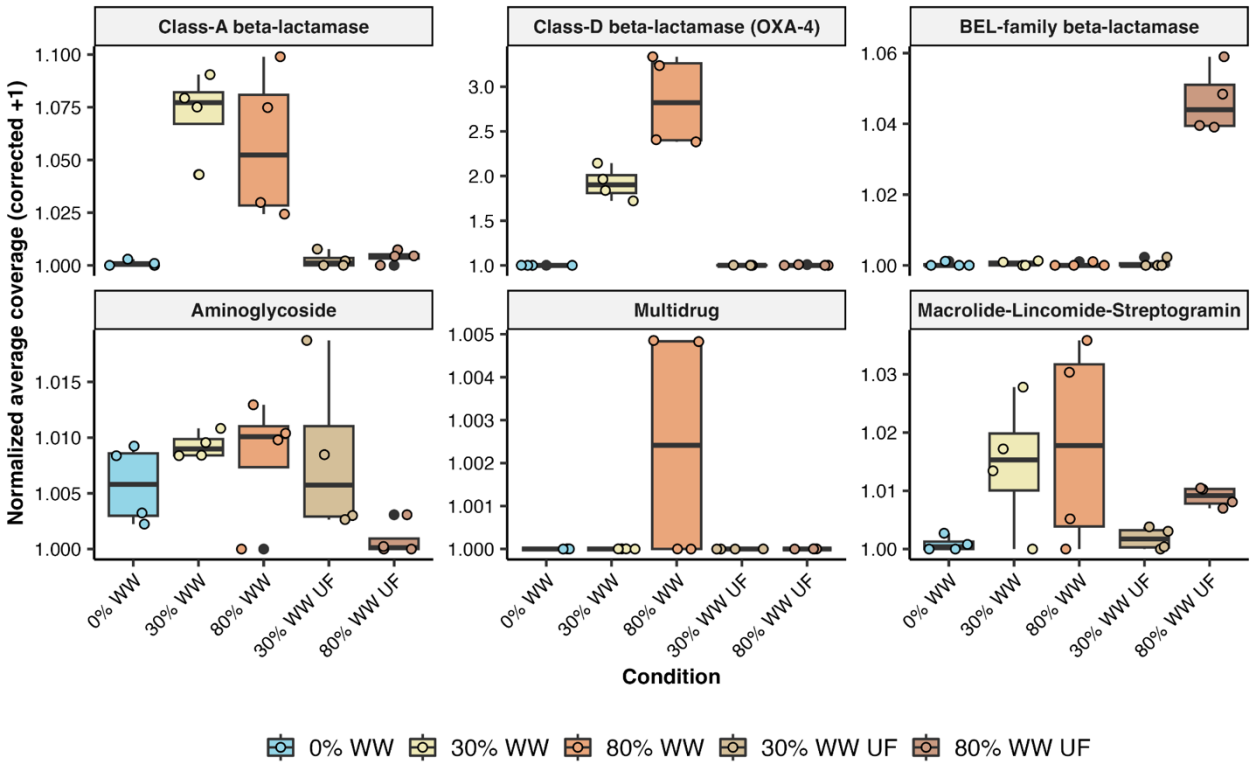

356 **Figure 4. Significant ARG classes using a metagenomic assembly-based approach.** The
357 corrected normalized average coverage of ARG cluster representatives identified using an
358 assembly-based ARG detection method. ARG clusters with significant differences in abundance
359 between at least one different treatment condition are displayed (adjusted p-values ≤ 0.05 using
360 Kruskal-Wallis test + Benjamini-Hochberg multiple hypothesis correction).

361

362 To quantify relative ARG abundances across treatment conditions, we mapped metagenomic
363 reads back to the 102 ARG cluster representatives. Ten ARG cluster representatives differed
364 significantly (Kruskal-Wallis test, $p < 0.05$) in abundance between at least one experimental
365 treatment condition (**Table S6**). In addition to two beta-lactam resistance ARGs, one each of the
366 multidrug, MLS, and aminoglycoside ARG representatives displayed the trend of increasing
367 abundance with increasing WW%. The fold change increase in metagenomic abundance was the
368 greatest for two beta-lactam resistance ARG clusters (Class-A beta-lactamase gene, $p = 0.0054$;
369 and a Class-D beta-lactamase bla OXA-4 gene, $p = 0.0054$; **Figure 4**). In contrast, a third beta-
370 lactam ARG (extended-spectrum BEL family beta-lactamase, p-value = 0.0488) displayed high
371 coverage exclusively in the 80% UF WW condition (**Figure 4**). These results suggest that the
372 abundance of this cluster of BEL family ARGs may be influenced by abiotic factors such as MPs,
373 the effects of which may have been outcompeted by biotic effects in the non-UF WW-grown
374 biofilms. Leveraging our metagenomic assembly-based approach, we examined genes localized
375 on the same metagenomic contig as the BEL family beta-lactamase hit. The BEL family beta-
376 lactamase is directly flanked by a *Pseudomonas* TniC resolvase. This TniC resolvase shares
377 100% sequence identity with a TniC resolvase (ADC80450.1) in integron/gene cassette systems
378 previously shown to be influenced by abiotic factors (heavy metal concentrations [63]. Although
379 the causality must be demonstrated, genetic mobility influenced by abiotic factors may contribute
380 to the observed abundance of BEL family beta-lactamases in 80% UF WW-grown biofilms.

381

382 Overall, our experimental design separated biotic and abiotic factors and shed light on the gene
383 family-specific mechanisms underlying how WWTP effluent may alter the resistome composition
384 of stream biofilms. Our combined results from short read mapping and assembly-based ARG
385 analysis generally aligned with the exception of the sulfonamide ARGs, which did not show a
386 significant difference in the assembly-based approach. This may be due to limitations in the
387 metagenomic assembly and highlights the value of using two different, complementary
388 approaches. For example, the significance of beta-lactamase ARGs identified via the short read-
389 based approach was also captured via the assembly-based approach. Notably, a consensus for
390 beta-lactamase abundance emerged from the comparison of our study to previous studies in
391 Switzerland [13] and globally [9,14,64,65]. Beta-lactamase ARGs consistently remain the most
392 abundant class of ARGs detected in WWTP effluent and aquatic environments [7,66–69]. Their
393 prevalence can be attributed to a variety of factors, including the early discovery and continued
394 widespread overuse of beta-lactam antibiotics for humans and animals [70,71]. However, the
395 unexpectedly high abundance of BEL family beta-lactamases exclusively in 80% UF WW samples
396 (**Figure 4)** prompted us to focus on beta-lactamases for further experimental investigation and
397 analysis of abiotic factors.

398 **Micropollutants as abiotic factors and their potential influence on ARG transfer**

399 We examined MP concentrations as abiotic factors capable of influencing gene family-specific
400 ARG abundances, such as the *sul1-4* and BEL family beta-lactamase ARGs showing
401 unexpectedly higher abundances in the UF WW compared to non-UF conditions (**Figure 3,**
402 **Figure 4)**. Based on previous chemical analysis by liquid chromatography-tandem mass
403 spectrometry [11], the MP concentrations measured in the flume biofilm samples increased with
404 increasing WW% (**Table S4**), but the concentrations of MPs extracted from biofilms did not
405 significantly differ between the UF and non-UF WW. Many of the antibiotics measured, including

406 sulfamethoxazole and sulfapyridine (**Table S4**), were present at concentrations less than or equal
407 to the limit of quantification in WW-grown biofilms. Among all antibiotics detected, the macrolide
408 clarithromycin exhibited the highest concentrations in 80% WW and 80% UF WW grown biofilms
409 (45-95 ng per mg biofilm, **Table S4**). In line with the general MP trends, clarithromycin
410 concentrations increased with WW% and did not vary significantly between UF and non-UF
411 treatments. In contrast, the metagenomic abundances of macrolide-lincosamide-streptogramin
412 (MLS) ARGs, which typically confer resistance to clarithromycin, were significantly lower in UF
413 than in non-UF conditions (**Figure 4**). This represents a case of an antibiotic-ARG pair where
414 ARG abundances did not correlate with the expected abiotic factor (clarithromycin). However, this
415 does not take into account the potential effects of other MPs which are not classified as antibiotics
416 but nonetheless influence ARG abundance [3].
417
418 A growing body of evidence indicates that many anthropogenic pollutants that do not have known
419 antimicrobial bioactivities nonetheless influence ARG transfer and proliferation [3,72–77].
420 However, there is generally a lack of knowledge on the mechanisms underlying how MPs without
421 antibiotic activities act as selective agents for ARG abundance. In our study, the 75 different MPs
422 measured [11] included artificial sweeteners, non-antibiotic pharmaceuticals, corrosion inhibitors,
423 and pesticides (**Table S4)**. Compared with the other compound classes, artificial sweeteners were
424 the most abundant MPs, with concentrations as high as μg/L detected in WW samples [11] (**Table**
425 **S4**). Notably, the artificial sweeteners measured in the biofilms (acesulfame K, cyclamate, and
426 saccharin) all contain sulfonamide moieties which are chemically analogous to the moieties found
427 in sulfonamide antibiotics (**Figure S8**). Sulfonamides were among the few ARG classes with
428 significantly greater abundances in UF WW-grown biofilms than in non-UF WW-grown biofilms
429 (**Figure 3**). These observations led us to speculate that abiotic factors, such as sulfonamide-
430 containing MPs, may play a role in promoting the abundance of such gene family-specific ARGs.

431 In support of this, several experimental studies have shown that artificial sweeteners promote
432 high rates of horizontal gene transfer and natural uptake of ARGs in bacteria [76,78]. Further work
433 has demonstrated that acesulfame-K and other artificial sweeteners directly enhance the rate and
434 quantity of horizontal plasmid-mediated transfers of *sul* genes [79]. Interestingly, a plasmid-
435 encoded microbial hydrolase capable of cleaving the sulfonamide moiety of acesulfame-K was
436 recently identified and shown to have a metallo beta-lactamase structural fold [80]. Taken
437 together, these findings prompted us to conduct a deeper functional investigation of beta-
438 lactamase fold genes whose abundance increased with WW%.

439

440 ***Planctomycetota* beta-lactamases display differential abundances in response to**
441 **sulfonamide-containing MPs and WWTP effluent**

442 To investigate the relationship between ARG abundances and sulfonamide-containing MPs, we
443 consulted previous reports of enrichment studies of activated sludge communities grown on
444 sulfonamide-containing MPs including artificial sweeteners [81,82]. Multiple independent
445 enrichment studies on acesulfame-K [82], saccharin [81], and cyclamate [81] reported significant
446 increases in the relative abundance of *Planctomycetota* and particularly the family
447 *Phycisphaeraceae*. Previously, Desiante et al. (2022) also identified significant differences in the
448 relative abundances of *Planctomycetota* and *Phycisphaeraceae* in biofilms grown in 80% WW
449 and 80% UF WW in two independent flume biofilm experiments ($\log_2$ -fold change > 4; $p < 0.05$).
450 We therefore conducted differential abundance analysis and observed statistically significant
451 differences in the *Planctomycetota* relative abundances between WW and UF WW treatments
452 (**Figure 5A**). Taxa assigned to the phylum *Planctomycetota* constitute up to 2.1% of the relative
453 abundance of our biofilm, WW, and stream water metagenomes, confirming previous reports of
454 the *Planctomycetota* as a numerically-important constituent both freshwater and wastewater
455 microbial communities [25,26,56]. Many *Phycisphaeraceae* are algae-associated with the

456 metabolic potential to impact the fitness of their algal hosts [83], but the current unculturability of
457 most planctomycetes limits our knowledge of linking their ARG genotypes to their phenotypes. To
458 address this knowledge gap, we chose to target *Phycisphaeraceae* ARGs for experimental
459 characterization.

460

461 Due to known challenges in planctomycete cultivation [56], we used heterologous expression
462 techniques to functionally validate two *Phycisphaeraceae* ARGs. We focused specifically on
463 *Phycisphaeraceae* beta-lactamases for four reasons: (1) the beta-lactamases were identified in
464 our ARG analysis as the most abundant and significantly-different class of ARGs affected by the
465 percentage of treated wastewater, (2) beta-lactamase fold enzymes were also previously
466 identified as plasmid-encoded enzymes active in the biotransformation of the sulfonamide MP
467 acesulfame-K [80], revealing the 'structural overlap' of a versatile metallo beta-lactamase fold
468 capable of cleaving both sulfonamide- and beta-lactam moieties, and (3) previous evidence of
469 sulfonamide cleavage in the sweetener cyclamate was shown by enzymes which were metal-
470 dependent hydrolases but their sequences were not determined [84]. Finally, (4) full-length
471 homologs with greater than 50% amino acid identity to the sulfonamide resistance genes *sul1-4*
472 were not detected in the *Phycisphaeraceae*. Since classical sulfonamide resistance genes were
473 lacking, we hypothesized that metallo beta-lactamase-fold enzymes may instead play an
474 overlooked role in sulfonamide cleavage in the *Phycisphaeraceae.*

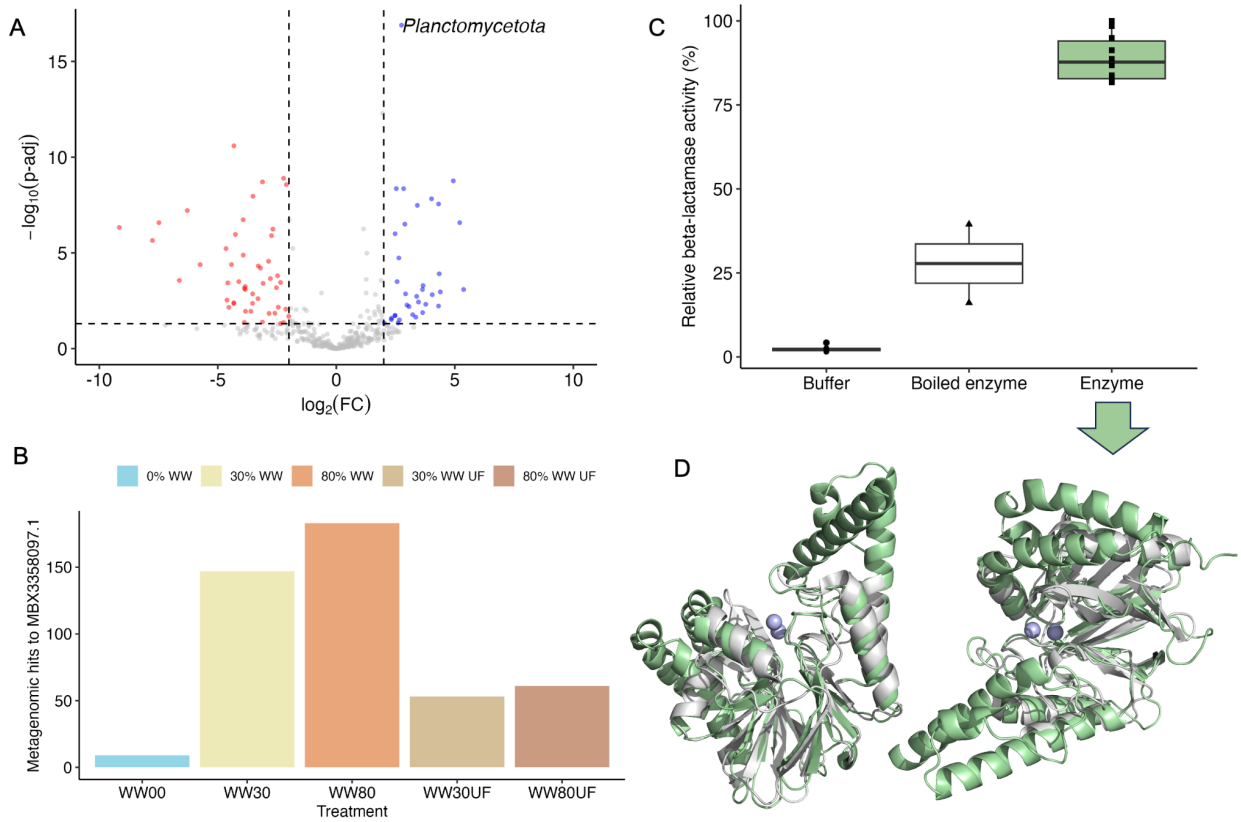

Figure 5. Functional characterization of an active *Planctomycetota* beta-lactamase. A) Volcano plot displaying the $\log_2$-fold change of differentially abundant taxa between WW30UF vs. WW30. B) Counts of hits showing significant homology to the putative beta-lactamase MBX3358097.1 in biofilm metagenomes. C) Purified enzyme assays demonstrated beta-lactamase activity of MBX3358097.1 with the colorimetric cephalosporin analog, nitrocefin, compared to boiled enzyme and buffer only controls. D) Two views of a high-confidence AlphaFold2 model (mean pLDDT = 96.5) of MBX3358097.1 structurally-aligned with its closest structural homolog in the Protein Data Bank (PDB100), as identified by FoldSeek [85] as of November 2023, the *Bacillus cereus* beta-lactamase (PDB ID: 3KNS).

488 **Functional characterization of a new beta-lactamase ARG from the *Planctomycetota***

489 To identify metallo-beta-lactamase fold enzymes assigned to the *Phycisphaeraceae*, we queried
490 the 75 metagenomes sequenced in this study as well as additional publicly-available
491 metagenomes from previous sulfonamide-containing MP enrichment studies [81,82]. Through
492 bioinformatic prioritization (Methods), we selected two full-length metallo beta-lactamase fold
493 protein hits from sulfonamide-enriched *Phycisphaeraceae* MAGs for functional characterization
494 [82]. The abundances of both proteins increased with increasing WW% (**Figure 5B** and **Figure**
495 **S9**). We heterologously expressed each of the *Phycisphaeraceae* genes in *E. coli.* One protein
496 did not express in *E. coli* and despite troubleshooting was not amenable to protein production or
497 purification with nickel-affinity chromatography. The second protein (MBX3358097.1) was soluble
498 and purified to homogeneity with an average yield of 500 µg/mL protein (**Figure S10**) therefore
499 we proceeded with the functional analysis of this protein. We tested the purified
500 *Phycisphaeraceae* protein for beta-lactamase activity and observed enzyme-mediated cleavage
501 of the cephalosporin analog, nitrocefin relative to boiled enzyme controls (**Figure 5C**). We next
502 tested its substrate specificity for sulfonamide-containing compounds. By high-performance liquid
503 chromatography analysis and comparison to authentic standards, we determined that the
504 *Phycisphaeraceae* enzyme did not biotransform the sulfonamide-containing MPs acesulfame-K,
505 saccharin, or cyclamate, nor did it transform sulfamethoxazole, thus disproving our hypothesis for
506 its role in sulfonamide cleavage. Nonetheless, this analysis resulted in the first biochemical
507 characterization of a new, active beta-lactamase from the *Phycisphaeraceae*.

508

509 MBX3358097.1 displayed a maximum 30% amino acid identity and between 20-50% query
510 coverage with proteins of known function in the UniProtKB-SwissProt [86] and the Beta-
511 Lactamase database (BLDB) [87]. These low sequence similarities limit reliable functional
512 annotation and beta-lactamase classification based on homology alone. Therefore, we generated

513 an AlphaFold2 model (Figure 5D, model available on GitHub) for the structural alignment and
514 identification of beta-lactamase subfamily specific motifs [88,89]. MBX3358097.1 encodes a zinc-
515 binding motif 2 (HxHxD**H**), which has a terminal histidine characteristic of the subclass B3 metallo
516 beta-lactamases. However, in another known motif 4, this enzyme contains the residues 'GD',
517 which are more characteristic of related glyoxalase II enzymes rather than B1-B3 family beta-
518 lactamases [88,89]. These results are suggestive of promiscuous activity or additional enzymatic
519 functions of MBX3358097.1 to investigate which are beyond the scope of this current study.
520 Nonetheless, this analysis highlights the benefits for structural modeling of metagenomic
521 sequences [90,91], particularly in cases where low sequence identity prevents reliable functional
522 annotation
523
524 There are few previous reports of ARGs from the phylum *Planctomycetota* [92]. Planctomycetes
525 were previously reported to have an unusual proteinaceous cell wall composition devoid of
526 peptidoglycan [93], however, later findings demonstrated that planctomycetes do indeed produce
527 peptidoglycan and are thus susceptible to cell-wall targeting antibiotics including beta-lactams
528 [94]. In fact, a study of six culturable planctomycetes revealed that all of the strains tested were
529 resistant to beta-lactam antibiotics although beta-lactamases could not be detected [95].
530 Importantly, MBX3358097.1 was also not detected by standard computational methods for
531 detecting ARGs, including queries to the SARG [43] and CARD [96] databases due to its low
532 sequence identity with known ARGs. This work therefore highlights the size of the knowledge gap
533 and invites further inquiry into the role of sequence-diverse ARGs from uncultivated
534 microorganisms and their contributions to environmental ARG reservoirs.
535
536
537

538 # Conclusions

539 Our results from a controlled flume system showed that WWTP effluent altered both the
540 microbiome and resistome composition of stream biofilms. Through ultrafiltration treatment of
541 WWTP effluent, we could attribute changes in ARG abundances primarily to biotic rather than
542 abiotic factors. However, the abundance of several gene family-specific ARGs, most notably
543 sulfonamides and beta-lactamases, suggested an influence by abiotic factors. We biochemically
544 characterized the beta-lactamase activity of a new *Phycisphaeraceae* protein with low sequence
545 identity to known ARGs. This provided proof-of-principle of a functional ARG from an uncultivated
546 microorganism that was overlooked by standard computational ARG detection methods. This
547 further highlights the need to characterize new ARGs from understudied taxa and to create a
548 more comprehensive ARG catalog for querying complex microbiomes. Overall, our study
549 exemplified a workflow to disentangle antibiotic resistance determinants in aquatic environments.

550 # List of abbreviations

ARGs	Antibiotic resistance genes
DNA	Deoxyribonucleic acid
MPs	Micropollutants
ORFs	Open reading frames
PCoA	Principal coordinate analysis
PCR	Polymerase chain reaction
rRNA	ribosomal Ribonucleic acid

SARG	Structured antibiotic resistance genes database
UF	Ultrafiltration
WW	Wastewater effluent
WWTPs	Wastewater treatment plants

Ethical approval and consent to participate

Not applicable

Availability of data and material

Metagenomic sequencing data generated during the current study have been deposited in the European Nucleotide Archive with the study accession code: PRJNA1008123. Scripts and additional data used in analysis and figures are available at:: https://github.com/MSM-group/AMR-ecoimpact-paper.

Competing interests

None

Funding

S.L.R. acknowledges support from the Swiss National Science Foundation (PZPGP2_209124), the Vontobel Foundation, and the Pierre Mercier Foundation. K.F. acknowledges the Swiss National Science Funding project no. 200021L_201006. H.B. and G.G. were supported by the ANTIVERSA project (BiodivERsA, European Union), Swiss National Science Foundation (Switzerland) grant no. 186531. Student funding for an advanced class at IHE Delft Institute of

Water Education was provided to M.A. through IHE Delft's DUPC2 programme project 'Supporting integrated and sustainable water management in Iraq through capacity development and research' grant number 109070.

Author's contributions

M.A. contributed to the conceptualization, methodology, investigation, writing—editing and revisions of the manuscript, visualization, and funding acquisition. M.S. contributed to conceptualization, methodology, visualization, investigation, data curation, writing—editing and revisions of the manuscript. M.E. contributed to the methodology, investigation, and revision and editing of the manuscript. G.G. contributed to methodology and editing and revision of the manuscript. H.B. contributed to the conceptualization, and editing and revision of the manuscript. P.N.L.L. contributed to the revision and editing of the manuscript and project administration. K.F. contributed to the conceptualization, revision and editing of the manuscript and funding acquisition. J.v.d.V. contributed to the methodology, writing- editing and revision of the manuscript and project administration. S.L.R contributed to conceptualization, methodology, Investigation, writing- editing and revision of the manuscript, visualization, project administration and funding acquisition.

Acknowledgements

We thank Dr. Bogdan Iorga for his export support in beta-lactamase classification and bioinformatic analysis. Robert Niederdorfer is acknowledged for his support and expertise in the metagenomic assembly through computational resources and collaboration with the Genetic Diversity Centre (GDC), ETH Zurich. We acknowledge Niklas Ferenc Trottmann for his training and support for the cloning, expression, and protein purification. We thank the Eawag Partnership Program together with the Institute of Water Education (IHE Delft) under the auspices of UNESCO for supporting the exchange of Mustafa Attrah to Eawag. We thank Elia Ceppi for assistance in

592 interpretation of chemical micropollutant data and Thierry Marti for support in biological
593 interpretation. We further acknowledge Stuart Dennis for his computational infrastructure support
594 at Eawag. We acknowledge the EcoImpact teams 1.0 and 2.0 for fruitful discussions as well as
595 conceptualizing and running the flume experiments which provided the samples necessary for
596 this study.

597 References

598 1. Marti E, Variatza E, Balcazar JL. The role of aquatic ecosystems as reservoirs of antibiotic
599 resistance. Trends Microbiol. 2014;22:36–41.

600 2. Singer AC, Shaw H, Rhodes V, Hart A. Review of Antimicrobial Resistance in the
601 Environment and Its Relevance to Environmental Regulators. Front Microbiol. 2016;7:1728.

602 3. Di Cesare A, Sabatino R, Sbaffi T, Fontaneto D, Brambilla D, Beghi A, et al. Anthropogenic
603 pollution drives the bacterial resistome in a complex freshwater ecosystem. Chemosphere.
604 2023;331:138800.

605 4. Bioavailability of potentially toxic elements influences antibiotic resistance gene and mobile
606 genetic element abundances in urban and rural soils. Sci Total Environ. 2022;847:157512.

607 5. Shallcross LJ, Davies DSC. Antibiotic overuse: a key driver of antimicrobial resistance. Br J
608 Gen Pract. 2014;64:604–5.

609 6. Alexander J, Hembach N, Schwartz T. Evaluation of antibiotic resistance dissemination by
610 wastewater treatment plant effluents with different catchment areas in Germany. Sci Rep.
611 2020;10:8952.

612 7. Rodriguez-Mozaz S, Chamorro S, Marti E, Huerta B, Gros M, Sànchez-Melsió A, et al.
613 Occurrence of antibiotics and antibiotic resistance genes in hospital and urban wastewaters and
614 their impact on the receiving river. Water Res. 2015;69:234–42.

615 8. Rogowska J, Cieszynska-Semenowicz M, Ratajczyk W, Wolska L. Micropollutants in treated
616 wastewater. Ambio. 2020;49:487–503.

617 9. Mukherjee M, Laird E, Gentry TJ, Brooks JP, Karthikeyan R. Increased Antimicrobial and
618 Multidrug Resistance Downstream of Wastewater Treatment Plants in an Urban Watershed.
619 Front Microbiol. 2021;12:657353.

620 10. Carles L, Wullschleger S, Joss A, Eggen RIL, Schirmer K, Schuwirth N, et al. Impact of
621 wastewater on the microbial diversity of periphyton and its tolerance to micropollutants in an
622 engineered flow-through channel system. Water Res. 2021;203:117486.

623 11. Desiante WL, Carles L, Wullschleger S, Joss A, Stamm C, Fenner K. Wastewater
624 microorganisms impact the micropollutant biotransformation potential of natural stream biofilms.
625 Water Res. 2022;217:118413.

626 12. Perveen S, Pablos C, Reynolds K, Stanley S, Marugán J. Growth and prevalence of
627 antibiotic-resistant bacteria in microplastic biofilm from wastewater treatment plant effluents. Sci
628 Total Environ. 2023;856:159024.

629 13. Lee J, Ju F, Beck K, Bürgmann H. Differential effects of wastewater treatment plant effluents
630 on the antibiotic resistomes of diverse river habitats. ISME J. 2023;17:1993–2002. Available
631 from: http://dx.doi.org/10.1038/s41396-023-01506-w.

632 14. Matviichuk O, Mondamert L, Geffroy C, Gaschet M, Dagot C, Labanowski J. River Biofilms
633 Microbiome and Resistome Responses to Wastewater Treatment Plant Effluents Containing
634 Antibiotics. Front Microbiol. 2022;13:795206.

635 15. Depetris A, Tagliavini G, Peter H, Kühl M, Holzner M, Battin TJ. Biophysical properties at
636 patch scale shape the metabolism of biofilm landscapes. NPJ Biofilms Microbiomes. 2022;8:5.

637 16. Romero F, Acuña V, Font C, Freixa A, Sabater S. Effects of multiple stressors on river
638 biofilms depend on the time scale. Sci Rep. 2019;9:15810.

639 17. Haenelt S, Richnow H-H, Müller JA, Musat N. Antibiotic resistance indicator genes in biofilm
640 and planktonic microbial communities after wastewater discharge. Front Microbiol.
641 2023;14:1252870.

642 18. Ju F, Lee J, Beck K, Zhang G, Gekenidis M-T, Hummerjohann J, et al. Phenotypic
643 Metagenomics tracks Wastewater-Associated Clinically Important Beta-lactam Resistant
644 Bacteria Invading River Habitats. Research Square. 2022; Available from:
645 https://www.researchsquare.com/article/rs-1589365/latest.pdf.

646 19. Reddington K, Eccles D, O'Grady J, Drown DM, Hansen LH, Nielsen TK, et al.
647 Metagenomic analysis of planktonic riverine microbial consortia using nanopore sequencing
648 reveals insight into river microbe taxonomy and function. Gigascience [Internet]. 2020;9.
649 Available from: http://dx.doi.org/10.1093/gigascience/giaa053.

650 20. Brumfield KD, Huq A, Colwell RR, Olds JL, Leddy MB. Microbial resolution of whole genome
651 shotgun and 16S amplicon metagenomic sequencing using publicly available NEON data. PLoS
652 One. 2020;15:e0228899.

653 21. Tremblay J, Singh K, Fern A, Kirton ES, He S, Woyke T, et al. Primer and platform effects
654 on 16S rRNA tag sequencing. Front Microbiol. 2015;6:771.

655 22. Klindworth A, Pruesse E, Schweer T, Peplies J, Quast C, Horn M, et al. Evaluation of
656 general 16S ribosomal RNA gene PCR primers for classical and next-generation sequencing-
657 based diversity studies. Nucleic Acids Res. 2013;41:e1.

23. Oyarzúa P, Bovio-Winkler P, Etchebehere C, Suárez-Ojeda ME. Microbial communities in an anammox reactor treating municipal wastewater at mainstream conditions: Practical implications of different molecular approaches. J Environ Chem Eng. 2021;9:106622.

24. Zhang Y, Zhao Z, Xu H, Wang L, Liu R, Jia X. Fate of antibiotic resistance genes and bacteria in a coupled water-processing system with wastewater treatment plants and constructed wetlands in coastal eco-industrial parks. Ecotoxicol Environ Saf. 2023;252:114606.

25. Andrei A-Ş, Salcher MM, Mehrshad M, Rychtecký P, Znachor P, Ghai R. Niche-directed evolution modulates genome architecture in freshwater *Planctomycetes*. ISME J. 2019;13:1056–71.

26. Cai X, Yao L, Sheng Q, Jiang L, Wang T, Dahlgren RA, et al. Influence of a biofilm bioreactor on water quality and microbial communities in a hypereutrophic urban river. Environ Technol. 2021;42:1452–60.

27. Carles, L., Wullschleger, S., Joss, A., Eggen, R.I.L., Schirmer, K., Schuwirth, N., Stamm, C., Tlili, A. Wastewater microorganisms impact microbial diversity and important ecological functions of stream periphyton, Water Res. 2022;225, 119119.

28. Li D, Liu C-M, Luo R, Sadakane K, Lam T-W. MEGAHIT: an ultra-fast single-node solution for large and complex metagenomics assembly via succinct de Bruijn graph. Bioinformatics. 2015;31:1674–6.

29. Hyatt D, Chen G-L, Locascio PF, Land ML, Larimer FW, Hauser LJ. Prodigal: prokaryotic gene recognition and translation initiation site identification. BMC Bioinformatics. 2010;11:119.

30. Salazar G, Ruscheweyh H-J, Hildebrand F, Acinas SG, Sunagawa S. mTAGs: taxonomic profiling using degenerate consensus reference sequences of ribosomal RNA genes. Bioinformatics. 2021;38:270–2.

31. Rognes T, Flouri T, Nichols B, Quince C, Mahé F. VSEARCH: a versatile open source tool for metagenomics. PeerJ. 2016;4:e2584.

32. Mansfeldt C, Achermann S, Men Y, Walser J-C, Villez K, Joss A, et al. Microbial residence time is a controlling parameter of the taxonomic composition and functional profile of microbial communities. ISME J. 2019;13:1589–601.

33. Buchfink B, Reuter K, Drost H-G. Sensitive protein alignments at tree-of-life scale using DIAMOND. Nat Methods. 2021;18:366–8.

34. Arango-Argoty G, Garner E, Pruden A, Heath LS, Vikesland P, Zhang L. DeepARG: a deep learning approach for predicting antibiotic resistance genes from metagenomic data. Microbiome. 2018;6:23.

35. Wickham H, Averick M, Bryan J, Chang W, McGowan L, François R, et al. Welcome to the tidyverse. J Open Source Softw. 2019;4:1686.

693 36. Robinson MD, Oshlack A. A scaling normalization method for differential expression
694 analysis of RNA-seq data. Genome Biol. 2010;11:R25.

695 37. Pereira MB, Wallroth M, Jonsson V, Kristiansson E. Comparison of normalization methods
696 for the analysis of metagenomic gene abundance data. BMC Genomics. 2018;19:274.

697 38. Robinson MD, McCarthy DJ, Smyth GK. edgeR: a Bioconductor package for differential
698 expression analysis of digital gene expression data. Bioinformatics. 2010;26:139–40.

699 39. Oksanen J, Kindt R, Legendre P, O'Hara B, Stevens MHH, Oksanen MJ, et al. The vegan
700 package. Community ecology package. 2007;10:719.

701 40. Paradis E, Claude J, Strimmer K. APE: Analyses of Phylogenetics and Evolution in R
702 language. Bioinformatics. 2004;20:289–90.

703 41. Benjamini Y, Hochberg Y. Controlling the false discovery rate: A practical and powerful
704 approach to multiple testing. J R Stat Soc. 1995;57:289–300.

705 42. McGinnis S, Madden TL. BLAST: at the core of a powerful and diverse set of sequence
706 analysis tools. Nucleic Acids Res. 2004;32:W20–5.

707 43. Yin X, Jiang X-T, Chai B, Li L, Yang Y, Cole JR, et al. ARGs-OAP v2.0 with an expanded
708 SARG database and Hidden Markov Models for enhancement characterization and
709 quantification of antibiotic resistance genes in environmental metagenomes. Bioinformatics.
710 2018;34:2263–70.

711 44. Lee J, Ju F, Maile-Moskowitz A, Beck K, Maccagnan A, McArdell CS, et al. Unraveling the
712 riverine antibiotic resistome: The downstream fate of anthropogenic inputs. Water Res.
713 2021;197:117050.

714 45. Fu L, Niu B, Zhu Z, Wu S, Li W. CD-HIT: accelerated for clustering the next-generation
715 sequencing data. Bioinformatics. 2012;28:3150–2.

716 46. Li W, Godzik A. Cd-hit: a fast program for clustering and comparing large sets of protein or
717 nucleotide sequences. Bioinformatics. 2006;22:1658–9.

718 47. Langmead B, Salzberg SL. Fast gapped-read alignment with Bowtie 2. Nat Methods.
719 2012;9:357–9.

720 48. Albertsen M, Hugenholtz P, Skarshewski A, Nielsen KL, Tyson GW, Nielsen PH. Genome
721 sequences of rare, uncultured bacteria obtained by differential coverage binning of multiple
722 metagenomes. Nat Biotechnol. 2013;31:533–8.

723 49. Camacho C, Coulouris G, Avagyan V, Ma N, Papadopoulos J, Bealer K, et al. BLAST+:
724 architecture and applications. BMC Bioinformatics. 2009;10:421.

725 50. Mirdita M, Schütze K, Moriwaki Y, Heo L, Ovchinnikov S, Steinegger M. ColabFold: making
726 protein folding accessible to all. Nat Methods. 2022;19:679–82.

727 51. Teufel F, Almagro Armenteros JJ, Johansen AR, Gíslason MH, Pihl SI, Tsirigos KD, et al.
728 SignalP 6.0 predicts all five types of signal peptides using protein language models. Nat
729 Biotechnol. 2022;40:1023–5.

730 52. Bradford MM. A Rapid and Sensitive Method for the Quantitation of Microgram Quantities of
731 Protein Utilizing the Principle of Protein-dye Binding. Analytical Biochem. 1976;72: 248-254.

732 53. O'Callaghan CH, Morris A, Kirby SM, Shingler AH. Novel method for detection of beta-
733 lactamases by using a chromogenic cephalosporin substrate. Antimicrob Agents Chemother.
734 1972;1:283–8.

735 54. Ryu BH, Ngo TD, Yoo W, Lee S, Kim B-Y, Lee E, et al. Biochemical and Structural Analysis
736 of a Novel Esterase from *Caulobacter crescentus* related to Penicillin-Binding Protein (PBP). Sci
737 Rep. 2016;6:37978.

738 55. Wu P, Chen J, Garlapati VK, Zhang X, Wani Victor Jenario F, Li X, et al. Novel insights into
739 Anammox-based processes: A critical review. Chem Eng J. 2022;444:136534.

740 56. Fuerst JA. Planctomycetes: Cell Structure, Origins and Biology. Springer Science &
741 Business Media; 2013.

742 57. Gionchetta G, Snead D, Semerad S, Beck K, Pruden A, Bürgmann H. Dynamics of antibiotic
743 resistance markers and Escherichia coli invasion in riverine heterotrophic biofilms facing
744 increasing heat and flow stagnation. Sci Total Environ. 2023;893:164658.

745 58. Ju F, Beck K, Yin X, Maccagnan A, McArdell CS, Singer HP, et al. Wastewater treatment
746 plant resistomes are shaped by bacterial composition, genetic exchange, and upregulated
747 expression in the effluent microbiomes. ISME J. 2019;13:346–60.

748 59. Gillings M, Boucher Y, Labbate M, Holmes A, Krishnan S, Holley M, et al. The evolution of
749 class 1 integrons and the rise of antibiotic resistance. J Bacteriol. 2008;190:5095–100.

750 60. Gillings MR, Gaze WH, Pruden A, Smalla K, Tiedje JM, Zhu Y-G. Using the class 1
751 integron-integrase gene as a proxy for anthropogenic pollution. ISME J. 2015;9:1269–79.

752 61. Tamames J, Cobo-Simón M, Puente-Sánchez F. Assessing the performance of different
753 approaches for functional and taxonomic annotation of metagenomes. BMC Genomics.
754 2019;20:960.

755 62. Peng Z, Mao Y, Zhang N, Zhang L, Wang Z, Han M. Utilizing metagenomic data and
756 bioinformatic tools for elucidating antibiotic resistance genes in environment. Front Environ Sci
757 Eng China. 2021;9. Available from:
758 https://www.frontiersin.org/articles/10.3389/fenvs.2021.757365/full

759 63. Rosewarne CP, Pettigrove V, Stokes HW, Parsons YM. Class 1 integrons in benthic
760 bacterial communities: abundance, association with Tn402-like transposition modules and
761 evidence for coselection with heavy-metal resistance. FEMS Microbiol Ecol. 2010;72:35–46.

762 64. Thornton CN, Tanner WD, VanDerslice JA, Brazelton WJ. Localized effect of treated
763 wastewater effluent on the resistome of an urban watershed. Gigascience. 2020;9. Available
764 from: http://dx.doi.org/10.1093/gigascience/giaa125

765 65. Czekalski N, Sigdel R, Birtel J, Matthews B, Bürgmann H. Does human activity impact the
766 natural antibiotic resistance background? Abundance of antibiotic resistance genes in 21 Swiss
767 lakes. Environ Int. 2015;81:45–55.

768 66. Laht M, Karkman A, Voolaid V, Ritz C, Tenson T, Virta M, et al. Abundances of tetracycline,
769 sulphonamide and beta-lactam antibiotic resistance genes in conventional wastewater treatment
770 plants (WWTPs) with different waste load. PLoS One. 2014;9:e103705.

771 67. Stoll C, Sidhu JPS, Tiehm A, Toze S. Prevalence of clinically relevant antibiotic resistance
772 genes in surface water samples collected from Germany and Australia. Environ Sci Technol.
773 2012;46:9716–26.

774 68. Osińska A, Korzeniewska E, Harnisz M, Felis E, Bajkacz S, Jachimowicz P, et al. Small-
775 scale wastewater treatment plants as a source of the dissemination of antibiotic resistance
776 genes in the aquatic environment. J Hazard Mater. 2020;381:121221.

777 69. Fadare FT, Okoh AI. The abundance of genes encoding ESBL, pAmpC and non-β-lactam
778 resistance in multidrug-resistant *Enterobacteriaceae* recovered from wastewater effluents. Front
779 Environ Sci Eng China [Internet]. 2021;9. Available from:
780 https://www.frontiersin.org/articles/10.3389/fenvs.2021.711950/full

781 70. Sta Ana KM, Madriaga J, Espino MP. β-Lactam antibiotics and antibiotic resistance in Asian
782 lakes and rivers: An overview of contamination, sources and detection methods. Environ Pollut.
783 2021;275:116624.

784 71. Agarwal V, Tiwari A, Varadwaj P. An Extensive Review on β-lactamase Enzymes and their
785 Inhibitors. Curr Med Chem. 2023;30:783–808.

786 72. Wang Y, Lu J, Zhang S, Li J, Mao L, Yuan Z, et al. Non-antibiotic pharmaceuticals promote
787 the transmission of multidrug resistance plasmids through intra- and intergenera conjugation.
788 ISME J. 2021;15:2493–508.

789 73. Kimbell LK, LaMartina EL, Kohls S, Wang Y, Newton RJ, McNamara PJ. Impact of corrosion
790 inhibitors on antibiotic resistance, metal resistance, and microbial communities in drinking water.
791 mSphere. 2023;e0030723.

792 74. Alderton I, Palmer BR, Heinemann JA, Pattis I, Weaver L, Gutiérrez-Ginés MJ, et al. The
793 role of emerging organic contaminants in the development of antimicrobial resistance. Emerging
794 Contaminants. 2021;7:160–71.

795 75. Qiu D, Ke M, Zhang Q, Zhang F, Lu T, Sun L, et al. Response of microbial antibiotic
796 resistance to pesticides: An emerging health threat. Sci Total Environ. 2022;850:158057.

797 76. Yu Z, Guo J. Non-caloric artificial sweeteners exhibit antimicrobial activity against bacteria
798 and promote bacterial evolution of antibiotic tolerance. J Hazard Mater. 2022;433:128840.

799 77. Zhang H, Song J, Zheng Z, Li T, Shi N, Han Y, et al. Fungicide exposure accelerated
800 horizontal transfer of antibiotic resistance genes via plasmid-mediated conjugation. Water Res.
801 2023;233:119789.

802 78. Yu Z, Wang Y, Henderson IR, Guo J. Artificial sweeteners stimulate horizontal transfer of
803 extracellular antibiotic resistance genes through natural transformation. ISME J. 2022;16:543–
804 54.

805 79. Li Z, Gao J, Guo Y, Cui Y, Wang Y, Duan W, et al. Enhancement of antibiotic resistance
806 dissemination by artificial sweetener acesulfame potassium: Insights from cell membrane,
807 enzyme, energy supply and transcriptomics. J Hazard Mater. 2022;422:126942.

808 80. Bonatelli ML, Rohwerder T, Popp D, Liu Y, Akay C, Schultz C, et al. Recently evolved
809 combination of unique sulfatase and amidase genes enables bacterial degradation of the
810 wastewater micropollutant acesulfame worldwide. Front Microbiol. 2023;14:1223838.

811 81. Deng Y, Wang Y, Xia Y, Zhang AN, Zhao Y, Zhang T. Genomic resolution of bacterial
812 populations in saccharin and cyclamate degradation. Sci Total Environ. 2019;658:357–66.

813 82. Huang Y, Deng Y, Law JC-F, Yang Y, Ding J, Leung KS-Y, et al. Acesulfame aerobic
814 biodegradation by enriched consortia and *Chelatococcus* spp.: Kinetics, transformation
815 products, and genomic characterization. Water Res. 2021;202:117454.

816 83. Rambo IM, Dombrowski N, Constant L, Erdner D, Baker BJ. Metabolic relationships of
817 uncultured bacteria associated with the microalgae *Gambierdiscus*. Environ Microbiol.
818 2020;22:1764–83.

819 84. Nimura T, Tokieda T, Yamaha T. Partial purification and some properties of cyclamate
820 sulfamatase. J Biochem. 1974;75:407–17.

821 85. van Kempen M, Kim SS, Tumescheit C, Mirdita M, Lee J, Gilchrist CLM, et al. Fast and
822 accurate protein structure search with Foldseek. Nat Biotechnol [Internet]. 2023; Available from:
823 http://dx.doi.org/10.1038/s41587-023-01773-0

824 86. UniProt Consortium. UniProt: the universal protein knowledgebase in 2021. Nucleic Acids
825 Res. 2021;49:D480–9.

826 87. Naas T, Oueslati S, Bonnin RA, Dabos ML, Zavala A, Dortet L, et al. Beta-lactamase
827 database (BLDB) - structure and function. J Enzyme Inhib Med Chem. 2017;32:917–9.

828 88. González JM. Visualizing the superfamily of metallo-β-lactamases through sequence
829 similarity network neighborhood connectivity analysis. Heliyon. 2021;7:e05867.

830 89. Denakpo E, Arlet G, Philippon A, Iorga BI. Metallo-β-lactamases. Metalloenzymes. Elsevier;
831 2024. p. 157–84.

832 90. Robinson SL. Structure-guided metagenome mining to tap microbial functional diversity.
833 Curr Opin Microbiol. 2023;76:102382.

834 91. Ruppé E, Ghozlane A, Tap J, Pons N, Alvarez A-S, Maziers N, et al. Prediction of the
835 intestinal resistome by a three-dimensional structure-based method. Nat Microbiol. 2019;4:112–
836 23.

837 92. Ivanova AA, Miroshnikov KK, Oshkin IY. Exploring Antibiotic Susceptibility, Resistome and
838 Mobilome Structure of Planctomycetes from *Gemmataceae* Family. Sustain Sci Pract Policy.
839 2021;13:5031.

840 93. König E, Schlesner H, Hirsch P. Cell wall studies on budding bacteria of the
841 *Planctomyces/Pasteuria* group and on a *Prosthecomicrobium* sp. Arch Microbiol.
842 1984;138:200–5.

843 94. Jeske O, Schüler M, Schumann P, Schneider A, Boedeker C, Jogler M, et al.
844 Planctomycetes do possess a peptidoglycan cell wall. Nat Commun. 2015;6:7116.

845 95. Cayrou C, Raoult D, Drancourt M. Broad-spectrum antibiotic resistance of Planctomycetes
846 organisms determined by Etest. J Antimicrob Chemother. 2010;65:2119–22.

847 96. Alcock BP, Huynh W, Chalil R, Smith KW, Raphenya AR, Wlodarski MA, et al. CARD 2023:
848 expanded curation, support for machine learning, and resistome prediction at the
849 Comprehensive Antibiotic Resistance Database. Nucleic Acids Res. 2023;51:D690–9.